Journal of Maps

ISSN: (Print) (Online) Journal homepage: www.tandfonline.com/journals/tjom20

Coupling morphometric analysis and soil erosion modeling for the characterization of the geomorphological setting in the surrounding of the archaeological site of Chimtou (Central Medjerda Valley, Tunisia)

Julia Pagels, Moheddine Chaouali, Corisande Fenwick, Philipp von Rummel & Wiebke Bebermeier

To cite this article: Julia Pagels, Moheddine Chaouali, Corisande Fenwick, Philipp von Rummel & Wiebke Bebermeier (2024) Coupling morphometric analysis and soil erosion modeling for the characterization of the geomorphological setting in the surrounding of the archaeological site of Chimtou (Central Medjerda Valley, Tunisia), Journal of Maps, 20:1, 2332369, DOI: 10.1080/17445647.2024.2332369

To link to this article: https://doi.org/10.1080/17445647.2024.2332369

JOURNAL OF MAPS
2024, VOL. 20, NO. 1, 2332369
https://doi.org/10.1080/17445647.2024.2332369

Taylor & Francis
Taylor & Francis Group

SCIENCE

OPEN ACCESS Check for updates

Coupling morphometric analysis and soil erosion modeling for the characterization of the geomorphological setting in the surrounding of the archaeological site of Chimtou (Central Medjerda Valley, Tunisia)

Julia Pagels [a], Moheddine Chaouali[b], Corisande Fenwick[c], Philipp von Rummel[d] and Wiebke Bebermeier [a]

[a]Institute of Geographical Sciences, Freie Universität Berlin, Berlin, Germany; [b]Institut National de Patrimoine, Tunis, Tunisia; [c]Institute of Archaeology, UCL, London, UK; [d]Deutsches Archäologisches Institut, Berlin, Germany

ABSTRACT

This study focuses on the characterization of the geomorphological setting in the hinterland of the archaeological sites of Chimtou and Bordj Hellal located in the central Medjerda Valley, North Tunisia. Our approach integrates the algorithm Geomorphons for semi-automatic landform classification with the soil erosion model Unit Stream Power-based Erosion Deposition (USPED), providing information on the intensity and regional distribution of erosional and depositional processes. Data from geomorphological field mapping provide a database for a ground-truth of the semi-automatic landform classification derived by the algorithm Geomorphons and complemented the database for the creation of a detailed map of the geomorphology in the hinterland of Chimtou. In line with the delineation of the spatial distribution of erosional and depositional processes, the results deepen the understanding of the geomorphology and the sediment routing of this region.

ARTICLE HISTORY
Received 3 September 2023
Revised 22 February 2024
Accepted 12 March 2024

KEYWORDS
Semi-automatic classification of landforms; USPED; Medjerda Valley; geoarchaeology; geomorphology

1. Introduction and background

The central Medjerda Valley in North Tunisia is known for its rich Numidian, Roman and medieval cultural heritage (Ardeleanu, 2021; Fenwick, 2022). Often called 'the granary of Rome', in antiquity, the region exported vast quantities of wheat to Rome and was densely settled with Roman towns, smaller settlements and farmsteads. It continued to be a major wheat-producer in the middle ages (Fenwick et al., 2022) and is today one of the most agriculturally productive regions in Tunisia (Jebari et al., 2012). Our study area is located in the hinterland of the archaeological sites of Chimtou (Roman *Simitthus*) and Bordj Hellal (possibly Roman *Thunusuda*), north of the Oued Medjerda. Chimtou is famed for its deposits of yellow marble (*marmor numidicum*) which were first quarried by the Numidian kings; under Roman rule. The marble was exported across the empire and used for prestige building projects such as the Pantheon in Rome (Beschaouch et al., 1993). The site was settled by the eighth century BCE (von Rummel et al., 2016) and became a large Roman and late antique town. Its later history is less clear but parts of the site were occupied in the ninth to twelfth centuries CE. Far less is known about Bordj Hellal, located 7 km downstream of Chimtou, the site has a pre-Roman phase, was fortified in the sixth century and seems to have been a large medieval town, seemingly displacing Chimtou in late antiquity.

Since 1965 excavations by the Institut National du Patrimoine and the German Archaeological Institute have focused on the marble quarries and the associated Roman work camp and the Numidian, Roman and late antique city (Beschaouch et al., 1993; Khanoussi et al., 1994; Mackensen & Baldus, 2005; von Rummel et al., 2019). In the early 2000s Christoph Zielhofer and Dominik Faust reconstructed fluvial dynamics of the Oued Medjerda, sedimentation rates in the floodplain and phases of geomorphic activity and stability in the Holocene (Faust & Zielhofer, 2002; Faust et al., 2004; Zielhofer & Faust, 2003).

In 2020, the joint project ISLAMAFR – 'Conquest, Ecology and Economy in Islamic North Africa: The Example of the Central Medjerda Valley' was established to explore the cultural, economic and landscape transformations of the central Medjerda Valley from late antiquity to the early medieval period (600–1000 CE) (Fenwick et al., 2022). Here we present results of the geoarchaeological work package whose overall aim is the reconstruction of paleoenvironmental

CONTACT Julia Pagels julia.pagels@fu-berlin.de Institute of Geographical Sciences, Freie Universität Berlin, Malteserstraße 74-100, 12249 Berlin, Germany

Supplemental map for this article can be accessed at https://doi.org/10.1080/17445647.2024.2332369.

conditions and landscape history between 600 and 1000 CE. As fieldwork was hindered by the Covid-19 pandemic until spring 2022, we first employed desk-based approaches to broaden our comprehension of the geomorphological characteristics of the study area and to identify suitable sediment archives for successive fieldwork, by addressing two research questions:

(a) What are the main geomorphological units of the study area and the respective predominate processes?

(b) How can the spatial distribution of erosion and deposition be characterized?

In this study we used the landform classification algorithm Geomorphons (Main Map G) (Jasiewicz & Stepinski, 2013) to get a first impression of the geomorphological characteristics of the hinterland of Chimtou and Bordj Hellal. This approach was also used by Frankl et al. (2016), who used this semi-automated landform classification to divided geomorphological regions in Montenegro. Yang et al. (2021) applied the geomorphon algorithm among other geomorphometric derivates to identify landform units in Turkey. Arosio et al. (2023) utilized Geomorphons as a tool to deepen their understanding while creating a geomorphological map in Ireland. The accuracy of the Geomorphons algorithm was validated by numerous studies, all highlighting that the geomorphon-based classification is a robust tool to identify geomorphological landforms (Atkinson et al., 2020; Gioia et al., 2021; Kramm et al., 2017; Libohova et al., 2016). Geomorphons is sensitive to pixel resolution and the search radius and archived results are less detailed compared to manual mapping (Libohova et al., 2016).

The Unit Stream Power-based Erosion Deposition model USPED (Main Map H) (Mitasova & Mitas, 2001; Mitasova et al., 1996a) identifies areas with potential of soil erosion or deposition (Mitasova et al., 2013) and was used to deepen our geomorphological process understanding in the hinterlands of Chimtou and Bordj Hellal. The USPED model is based on the (R)USLE models, but additionally computes soil deposition (Mitasova et al., 1996b). Studies comparing the USPED model against other established models (RUSLE and RUSLE3D) and against field data concluded the feasibility of the USPED model to estimate the spatial distribution of soil erosion and deposition realistically (Aiello et al., 2015; Arrebei et al., 2020; Ben Ameur et al., 2021; Lazzari et al., 2015; Sandström et al., 2023; Warren & Ruzycki, 2022).

Data from geomorphological field mapping in March and September 2022 constitute a database for a ground-truth and result in line with information derived from geological maps and digital elevation models (DEM) in the composition of a geomorphological map for the hinterlands of Chimtou and Bordj Hellal (Main Map E).

2. Study area

2.1. Geological setting and hydrogeography

The Medjerda Valley is a graben located between the Tellian fold-and-thrust belt, encompassing the Kroumir mountains and the Northern Atlas belt, which includes the Dorsal mountain range (Khelil et al., 2019, 2021) (Map B). Halokinetic movements of Triassic salt bodies (Khelil et al., 2021) further determine the overall structural layout of major landforms. The Kroumir mountains, stretching from the coastal plain in the North to the northern margin of the study area, gently transition into the Fernana wedge-top basin, filled with Late Miocene deposits composed of clays, sandstones and conglomerates (Main Map C).

In the north-east the Djebel el Haïrech is found, consisting of schist and sandstone of Triassic age, with associated Liassic marble deposits. The Djebel el Haïrech is separated from the Fernana wedge-top basin by the Djebel Chouichia, an escarpment composed of rocks of late Cretaceous age which is framed by two faults. The Medjerda Valley itself is filled with Upper Miocene to Holocene sediments (Faust & Zielhofer, 2002; Khelil et al., 2021).

The Oued Medjerda is the main, perennial and meandering river in Tunisia and the main water source in North Tunisia (Rodier et al., 1981) (Main Map D). It originates in the Atlas Mountains in East Algeria and flows into the Mediterranean Sea north of Tunis. The watershed of the Oued Medjerda encompasses c. 22.000 km². Sedimentation rates, derived from the alluvial plain of the Oued Medjerda are sensitive to the North Atlantic climate behavior, e. g. the North Atlantic cooling from 4.7 ka onwards is reflected in the sedimentation rates (Faust & Wolf, 2017; Faust et al., 2004). Sediment records point to soil formation and an incision of the Oued Medjerda during the Roman era, while during the post-Roman period, extreme flooding and an increase in morphodynamics prevail (Zielhofer & Faust, 2003).

2.2. Climate

Climatically the Medjerda Valley is located in a transitional zone between the two framing mountain ranges in the North and South. The climate of the valley corresponds to the Mediterranean subtropics with hot and dry summers and humid winters.

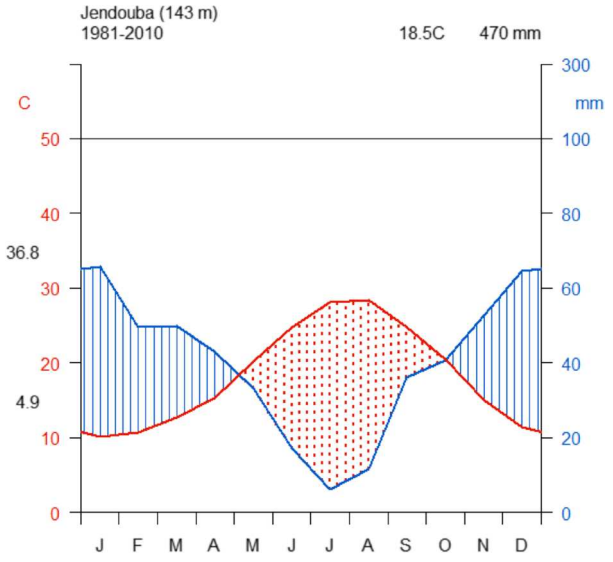

Figure 1. Climate diagram of Jendouba, Tunisia (Data: INM, 2018).

After Gießner (1984) there is a precipitation gradient with decreasing precipitation from north to south. While the Kroumir mountains in the North are characterized by Mediterranean-humid conditions with a mean annual precipitation range between 600 and 800 mm, the Dorsal mountains in the South are classified to the Mediterranean semiarid to semi humid zone with mean annual precipitation amounts up to 400 mm (Gießner, 1984). The Jendouba climate station, located in the center of the study area, shows annual average temperature of 18.5°C for the period of 1981–2010 and mean annual precipitation averages of 470 mm (Figure 1).

2.3. Vegetation and land-use

The Medjerda Valley is a traditional agricultural area, where today cereals and olives are the main crop. The earliest known settlement and agricultural use of the Valley is now attested archaeologically at Chimtou from the eighth century BCE (von Rummel et al., 2016). With increasing anthropogenic influence, the natural Mediterranean pine forests with *Pinus halpensis* and shrubs of *Quercus ilex* occur today only fragmented in the mountain ranges (Gaussen & Vernet, 1958; Gießner, 1984; Menasria et al., 2022; Zielhofer & Faust, 2003).

3. Methods

In this study we couple the semi-automated landform algorithm Geomorphons (Jasiewicz & Stepinski, 2013), the soil erosion model USPED (Mitasova et al., 1996a, 1996b) with geomorphological field mapping to characterize the geomorphological setting of the study area and spatial dynamics of sediment routing. Further, the slope and a river elevation model (REM) were derived on the base of the digital elevation model (DEM). The geological map 1:50.000 (Mathieu et al., 1952) was digitized for the extend of the study area. All data underwent ground truthing during field trips in March and September 2022 and were compiled in a Geomorphological Map (Main Map E).

3.1. Geomorphons algorithm

The Geomorphons algorithm by Jasiewicz and Stepinski (2013) classifies landforms based on digital elevation data. This algorithm uses a local binary ternary pattern recognition approach where for each pixel of a DEM a morphological terrain type is assigned. This machine vision approach returns a geomorphic raster image with 10 (most popular) terrestrial landforms constructed from the eight neighbors of a cell (Jasiewicz & Stepinski, 2013).

We used the DEM from the TanDEM-X mission with an independent pixel spacing of 0.4 arcsec (~12 m at equator) (Wessel, 2018) with the r.geomorphon module in GRASS GIS. The DEM was prepared by smoothing the waterbodies and calculating the orthometric height from the TanDEM X data (given in ellipsoidal height) using the global EGM96 geoid (The EOC Geoservice Team, n.d.). After testing different configurations, 50 cells was selected for the outer search radius, 10 cells for the inner search radius and 1° for the flatness threshold.

3.2. USPED model

The USPED model is an adaptation of the Universal Soil Loss Equation (USLE), that additionally takes the sediment transport capacity of a steady state overland flow to compute the net erosion and deposition (Mitasova & Mitas, 2001; Mitasova et al., 1996a, 2013). The USPED model multiplies five input variables characterizing topography, land use, soil characteristics, conservation measures and the rainfall erosivity to calculate the estimate sediment flow T in t m ha^{-1} yr^{-1} at sediment transport capacity for each pixel:

$$T = R \times K \times C \times LST \times P$$

R is the rainfall erosivity factor [MJ mm ha^{-1} h^{-1} yr^{-1}], K is the soil erosivity factor [t ha h ha^{-1} MJ^{-1} mm^{-1}], C is the land cover factor [dimensionless], LST is the sediment transport capacity [m^2 m^{-1}] and P is the prevention measures factor [dimensionless].

The divergence of the sediment flow T computes the net erosion/deposition D [t ha^{-1} yr^{-1}] to predict spatial patterns of erosion and deposition (Mitasova et al., 1996a, 1999, 2013):

$$D = \frac{\partial(T \cos\alpha)}{\partial x} + \frac{\partial(T \sin\alpha)}{\partial y}$$

where α in degree is the direction of flow as aspect of the terrain surface. A positive D shows the potential for soil deposition and a negative D marks the potential for erosion (Mitasova et al., 1996a).

The model area covers the entire Medjerda Valley and 22.5% of the watershed of the Oued Medjerda (a map can be found in the supplementary material). In this paper, results are clipped to a study area of 115 km^2 corresponding to the hinterland of Chimtou and Bordj Hellal, representing 2.35% of the model area.

3.2.1. R-factor

Rainfall Erosivity (R) gives a measure of the erosive force caused by precipitation. Benavidez et al. (2018) reviewed various approaches to calculate the R-factor and highlighted the well-established practice of utilizing monthly precipitation data in regions where high-resolution data are lacking. Due to the lack of long-term daily precipitation data in Tunisia we therefore applied the approach based on monthly precipitation data after Ferro et al. (1999). Input data was provided by the Institut national de la Météorologie Tunisie (Institut National de la Météorologie [INM], 2018) for the period 1981–2010. All available climate stations in North Tunisia were considered for this analysis (Figure 2).

The R-factor in MJ mm ha^{-1} h^{-1} yr^{-1} is a multiplication of the modified Fournier index (MFI):

$$R = 0.6120 \times MFI^{1.56}$$

$$MFI = \sum_{i=1}^{12} \frac{P_i^2}{P}$$

MFI is a summation of the monthly precipitation P_i in mm and the annual precipitation P in mm over a 12-month cycle (Arnoldus, 1977, 1980). The R-factor, calculated for altogether 17 climate stations, was interpolated from the original point source to continuous raster data applying inverse distance weighting (IDW) (Philip & Watson, 1985). A map of the climate stations can be found in the supplementary material.

3.2.2. K-factor

The soil erodibility factor (K) refers to the susceptibility of a soil to erode, given in t ha h ha^{-1} MJ^{-1} mm^{-1}. It was calculated after Sharpley and Williams (1990), with soil texture and organic carbon content of the top soil layer as input data. We used data from the SoilGrids model provided by the International Soil Reference and Information Centre (ISRIC) and applied the trapezoidal rule on the first 30 cm for the different soil properties (Sand SAN, Silt SIL, Clay CLA, Organic Carbon Content OC) (Hengl et al., 2017). K was estimated after Sharpley and Williams (1990):

$$K = 0.1317 \times (0.2 + 0.3 \exp(-0.0256 \times SAN(1 - SIL \div 100))) \times \left(\frac{SIL}{CLA + SIL}\right)^{0.3} \times \left(1 - \frac{0.25 \times OC}{OC + \exp(3.72 - 2.95 \times OC)}\right) \times \left(1 - \frac{0.7 \times (1 - SAN \div 100)}{(1 - SAN \div 100) + \exp(-5.51 + 22.9 \times (1 - SAN \div 100))}\right)$$

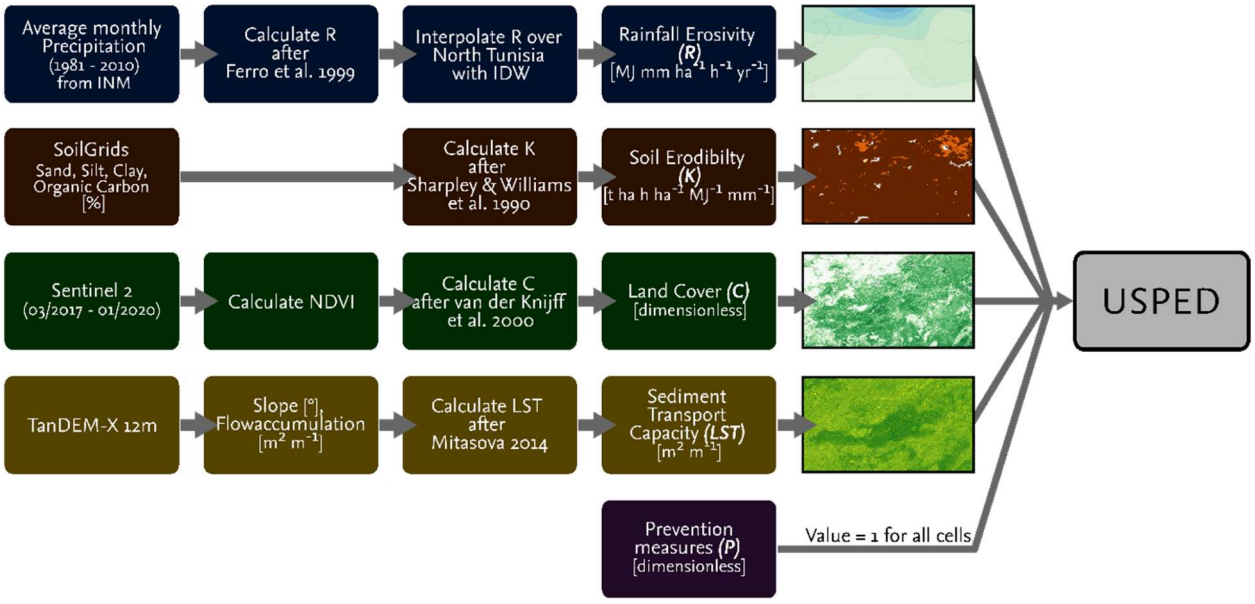

Figure 2. Workflow diagram including input datasets and methods applied for the implementation of the USPED model.

3.2.3. C-factor

The land cover factor (C) is used to reflect the effect of cropping and management practices on erosion rates. It was calculated after van der Knijff et al. (2000) using the Normalized Difference Vegetation Index (NDVI), where α has a value of 2 and β has a value of 1:

$$C = -\alpha \times \frac{NDVI}{(\beta - NDVI)}$$

We computed the median NDVI from all Sentinel 2 images from March 2017 to January 2022 with less than 10% cloud coverage using Google Earth Engine.

3.2.4. LST-factor

The sediment transport capacity (LST) of overland flow is a three-dimensional topographic factor. This is calculated from the slope length and slope angle, here from the TanDEM-X data. The LST factor was calculated after Mitasova et al. (2014).

3.2.5. P-factor

The prevention measures factor (P) offers an option to include soil conservation methods such as contour farming, stone walls or grass margins. For the central Medjerda Valley no prevention measures were known, accordingly we applied 1.0 as a factor.

4. Results and discussion

4.1. USPED

In the study area, low depositional conditions are prevailing as indicated by a positive mean net erosion/deposition of 4.26 t ha^{-1} yr^{-1}. Deposition takes place in the alluvial plain, the southern foot slopes of the Djebel Haïrech and the foot slopes north of the Djebel Chimtou (Figure 3). High erosion rates are found in the valleys and along depth contours on slopes. In the alluvial plain, high erosion rates occur along the river course of the Oued Medjerda, its tributaries and along depth contours, draining in the Medjerda River. The ridges of the Djebel Chimtou and Djebel el Haïrech show low erosion. The archaeological sites Chimtou and Bordj Hellal are both located in areas where stable to low rearrangement processes are calculated.

For the parametrization of the USPED model, limitations in the availability of spatially and temporal high-resolution data resulted in the use of input data of a comparably coarse resolution. In addition, validation with measured soil erosion data (e. g. sediment yield for rivers) was not possible due to lack of available data. These challenges have been highlighted in recent studies modeling soil erosion rates in Tunisia (Jebari et al., 2010; Jemai et al., 2021). The main methods applied in this study for the calculation of input variables (C, K and R factor) were successfully tested and

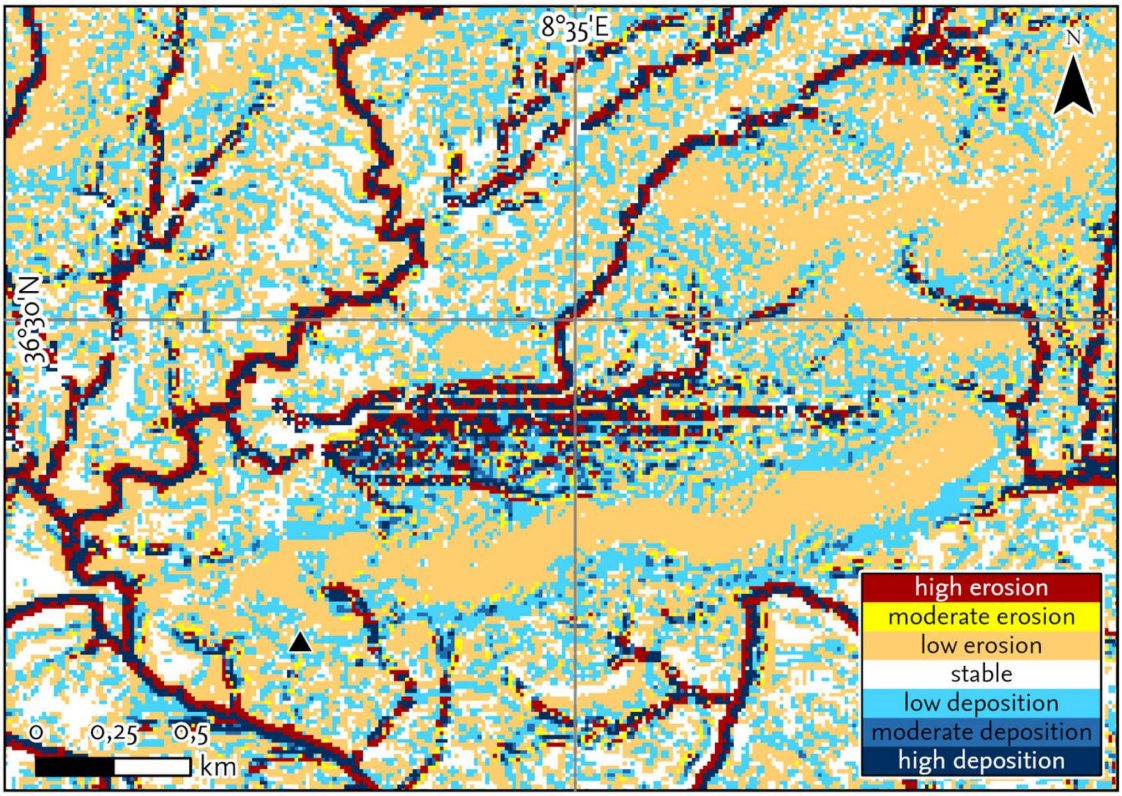

Figure 3. Detail from the USPED model around the Djebel Chimtou. Map shows predicted annual soil loss in t ha^{-1} yr^{-1} categorized as high erosion (<−10), moderate erosion (−5 to −10), low erosion (−5 to −0.1), stable conditions (−0.1 to 0.1), low deposition (0.1 to 5), moderate deposition (5 to 10) and high deposition (>10).

applied in the framework of other studies in North Tunisia (Kefi et al., 2012; Menasria et al., 2022; Mosbahi & Benabdallah, 2020). Studies by Benavidez et al. (2018) and Majhi et al. (2021) reviewed communally used calculations for the R-, K-, C- and P-factor for soil erosion models, emphasizing the complexity of choosing the most appropriate method for calculating input factors and the wide range of results with different calculations. We choose our input factor calculations based on data availability and calculations successfully used in other regional studies. As the focus of our study is not the exact quantitative calculation of erosion and deposition rates, but rather the qualitative designation of areas being mainly characterized by erosion, transport and deposition we evaluate the model parametrization and results as robust and suitable for the purpose of this study. Our assessment is supported by field mapping, whose results are in line with the model output, indicating a strong consistency between the model and reality.

4.2. Geomorphological units

The geomorphological setting of the study area can be delineated in six main units, which are presented in Main Map E.

4.2.1. Geomorphological Unit 1 – alluvial plain

The alluvial plain of the Oued Medjerda covers the entire area of lower altitude between 110 and 250 m above sea level. Steep slopes are associated with the meander belt of the Oued Medjerda and the river courses of its tributaries (Oued Melah in the North and Oued Meliz in the South). The sediment architecture of the alluvial plain consists of Holocene alluvial deposits (Zielhofer & Faust, 2003), in which the Oued Medjerda has incised.

The alluvial plain is predominantly characterized by stable conditions, with low erosion and deposition rates, and can in general be interpreted as a depositional environment. Here erosion occurs predominantly along fluvial channels of the tributaries of the Oued Medjerda and in the course of depth contours. West of the ridge of Djebel Chimtou, three tributary streams (the Oued Meliz, Oued Melah and Oued Rarai) enter the alluvial plain of the Oued Medjerda. The location of the Roman settlement of Chimtou at a slightly higher elevation close to the Djebel Chimtou, provides a certain protection against flood events.

The results of the USPED model show that the area north of the Djebel Chimtou represents a cluster of high erosion and deposition rates (Figure 3), pointing to the highly dynamic characteristics of this region, which probably are connected to the valley entering the area from the North. This area operates as a sediment trap for sediments originating from the valley between the Djebel Chouichia (Unit 5) and the Djebel el Haïrech (Unit 2).

The Geomorphons classification returned most of the floodplain as flat. Anthropogenic structures such as roads, railway and field edge boundaries represent residuals, as modern anthropogenic features were not removed from the DEM prior the Geomorphons analysis.

The Oued Medjerda is a dynamically meandering river, as numerous paleochannels and terrace levels indicate (REM, Main Map D). Zielhofer and Faust (2003) mapped paleochannels of the Oued Medjerda in the hinterland of Chimtou. In this study we identified additional paleochannels east of Chimtou based on the REM and field mapping.

Beside geographical evidence, archaeological research provides evidence for phases of increased fluvial dynamics of the Oued Medjerda. The Roman bridge over the Oued Medjerda was one of the largest Roman bridges in North Africa. It was completed in 112 CE, later repaired multiple times in response to the changing watercourse and flood events, until it finally collapsed in the fourth or fifth century CE (Hess et al., 2017). The fluvial dynamics in the vicinity of Chimtou are also reflected in the relocation of the river mouth of the Oued Melah. During the Roman period, the Oued Melah flowed through the settlement and joined the Oued Medjerda east of the ancient bridge (Hess et al., 2017), until in a later period, its lower course was cut by a meander of the Oued Medjerda, so that the Oued Melah nowadays joins the Oued Medjerda north of the site.

4.2.2. Geomorphological Unit 2 – escarpment, slopes and ridges of Djebel el Haïrech

The Djebel el Haïrech, framing the Medjerda valley in the north, is divided in two subunits: (2a) comprise the south-facing escarpment, which boarders the alluvial plain to the north and (2b) the northern slopes and ridges of Djebel el Haïrech located north of it. The geology of Djebel el Haïrech is made out of Triassic schist and sandstone with embedded Liassic marble deposits cropping out at selected locations. Its topography is small chambered with numerous summits and ridges. The slopes of the Djebel el Haïrech are intersected by erosional gullies, with correlating alluvial fans located at the footslopes, which partly overlap each other (Main Map E). On the south and south-west facing slopes foot slope deposits developed, which are not found on the north facing slopes presumably due to the shorter slope length (Figure 4). From low erosive conditions on the ridges, the dynamics change to a depositional environment in the foot slopes. In the high elevation areas where forests are found stable conditions prevail. The pronounced valley Bled es Zoubia represents an own geomorphological unit and is described in Section 4.2.3. The site Bordj Hellal is located at the edge of an

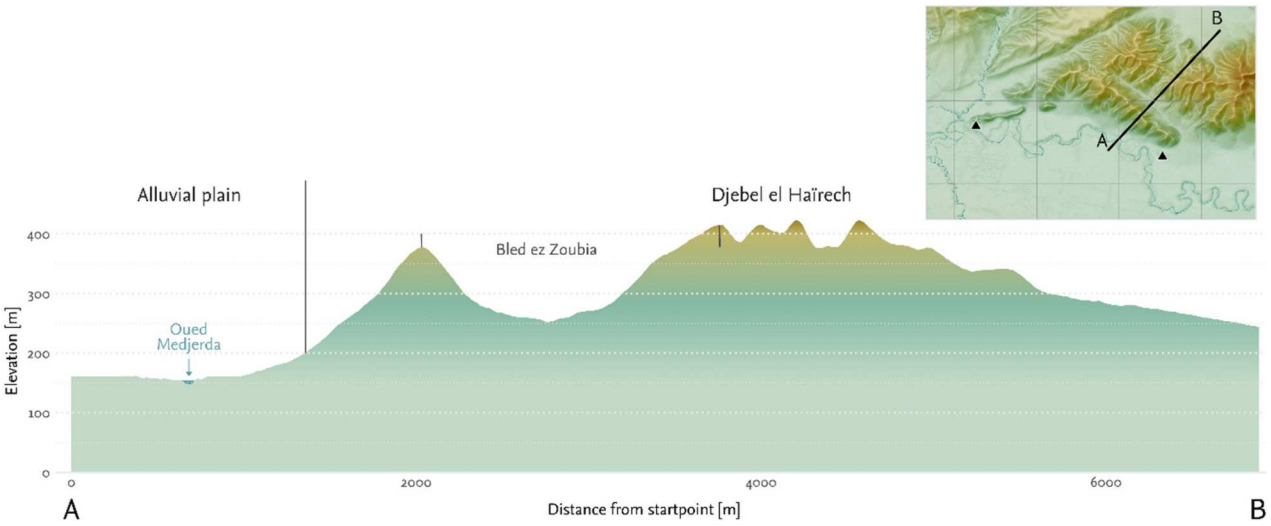

Figure 4. Cross section over the Djebel el Haïrech (Unit 2) including the Bled ez Zoubia valley (Unit 4) (Data: TanDEM-X 12m).

Figure 5. Picture from the bedrock present at the ridge of Djebel el Haïrech (left) and picture of an outcrop in the Bled ez Zoubia valley (right).

alluvial fan corresponding to an elevated topography that provides a certain protection against floods.

4.2.3. Geomorphological Unit 3 – valley Bled ez Zoubia

The north-east to south-west-oriented valley within the Djebel el Haïrech is referred to as Bled ez Zoubia. At its outlet, a wide alluvial fan is situated that extends into the floodplain of the Oued Medjerda. The valley itself is characterized by lateral valleys depositing small alluvial fans, which partly intersect with each other. Along the slopes channel erosion can be observed from the USPED model (Main Map H) and geomorphological field mapping. At the ridges, frequently outcropping bedrock is found (Figure 5). In the valley, low erosion and low deposition rates dominate. Stable conditions only cover small areas which can be referred to as sediment transfer zone. The alluvial fans are intersected by fluvial channels, whose banks expose the underlying sediment stratigraphy, which frequently comprise alternating layers of loam and inlaid gravel layers (Figure 5).

4.2.4. Geomorphological Unit 4 – ridge Djebel Chimtou

Djebel Chimtou is the source area of the yellow marble, exploited between the second century BCE and the fourth/fifth centuries CE by the Romans and again in the nineteenth and twentieth centuries. The ridge and the upper slopes of the Djebel Chimtou are covered by rounded marble blocks with sporadic shrubs growing in between. The USPED model returned low erosion rates at the slopes of the Djebel Chimtou, which aligns with the field observation that soils only occur in small depressions between the marble outcrops (Figure 6 – Unit 4). The foot slopes are characterized as depositional environment.

4.2.5. Geomorphological Unit 5 – escarpment Djebel Chouichia

Djebel Chouichia is an escarpment located in north-western direction of the Djebel el Haïrech (Unit 2). Its lithology is composed of tertiary and cretaceous limestones and marls. It is delineated from the

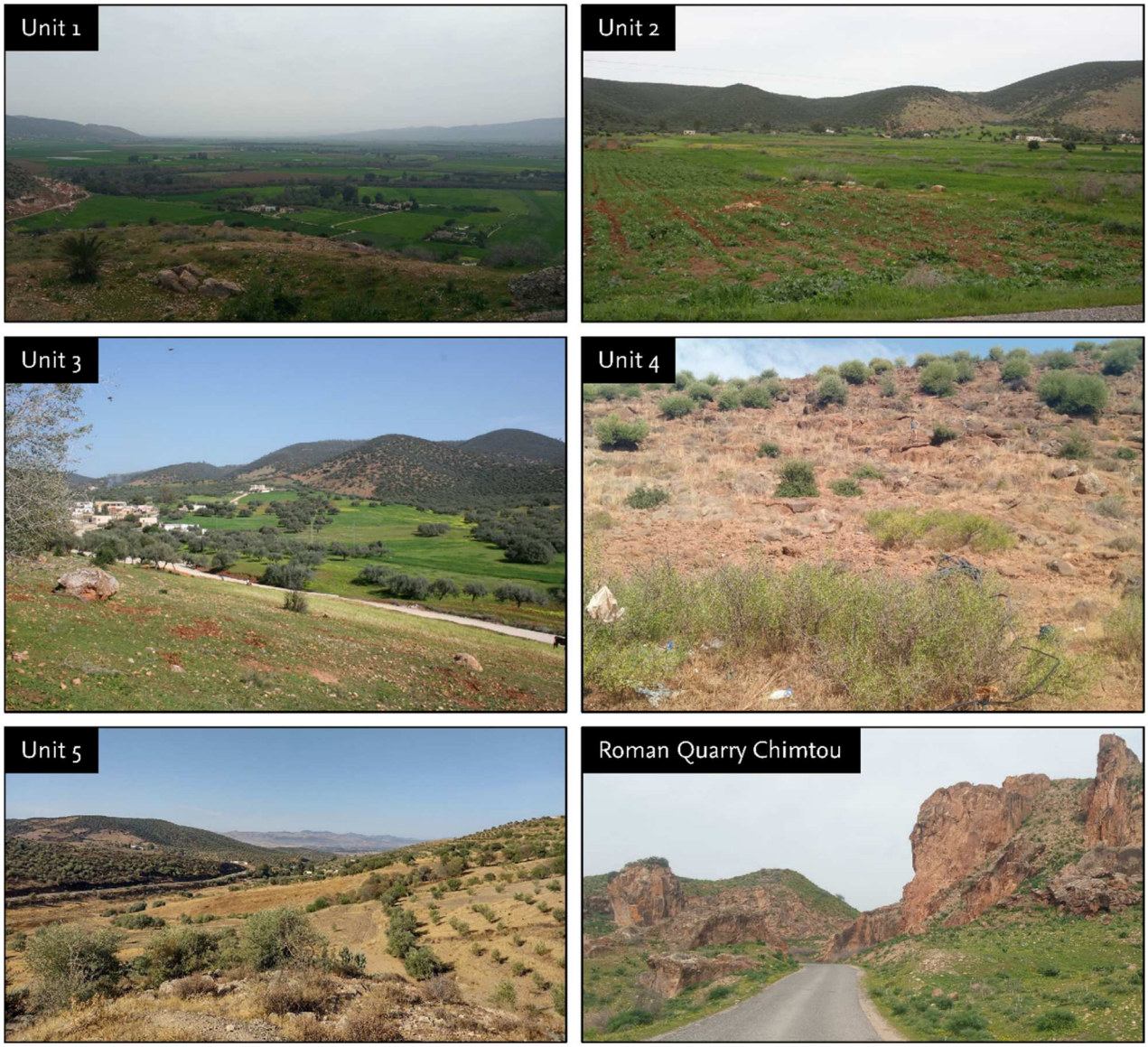

Figure 6. Pictures from the geomorphological units and one of the roman quarries in Chimtou expanded in the nineteenth and twentieth century (Photos: Unit 1–4 and Roman Quarry Chimtou: J. Pagels, Unit 5: W. Bebermeier).

adjacent Fernana wedge-top deposits (Unit 6) by its differing bedrock (Main Map C). Its main topographic characteristic is the steep south-east exposed slopes. Between Djebel Chouichia and Djebel el Haïrech a pronounced valley has formed.

4.2.6. Geomorphological Unit 6 – southern outer margin of the Fernana wedge-top basin

The Kroumir mountains are located in the North-western part of the study area and dip gently in toward the Medjerda valley. After Khelil et al. (2021) the part of the Kroumir mountains in the study area belongs to the Fernana wedge-top basin, which is intersected by a valley through which the tributary Oued Melah flows. Channel erosion is found along the slopes and valleys. Similar to the Djebel el Haïrech, low erosion rates are computed for the ridges. As the Fernana wedge-top basin in the study area is used for agriculture, there is scarcely any tree cover. Overall the slopes of this unit are characterized by alternating low erosion and deposition rates, while the latter correspond to areas of low slope gradient.

5. Conclusions

This study has produced the first detailed geomorphological map (Main Map E) of the hinterland of Chimtou and Bordj Hellal, by integrating basic derivates of digital elevation data (Geomorphons, REM, Slope), thematic maps of the study area (geology) and subsequent fieldwork as measure of ground truthing. By using the USPED model, we increased the understanding of the spatial pattern of sediment routing in the study area. Beyond that altogether six geomorphological units were identified and characterized.

Erosion and deposition rates vary across different units, with erosion being more pronounced in certain areas such as valleys and slopes, while deposition or stable conditions frequently occur at the foot slopes.

In the alluvial plain, stable conditions prevail with linear erosion along the fluvial channel. The slopes of the Djebel Chimtou and Djebel el Haïrech are predominantly characterized by erosion, resulting in the formation of foot slope deposits on the south-east facing slopes. The Bled ez Zoubia valley deposits a wide alluvial fan that extends into the alluvial plain, while the valley itself is represented by sediment transport. In this valley erosion rates show a dependency from the slope gradient and the tree cover at the slope.

Results gained from the digital mapping of the region were successfully applied to identify suitable sediment archives, here paleochannels of the Oued Medjerda around Chimtou and the south-east facing foot slopes for a successive geoarchaeological reconstruction of paleoenvironmental conditions and landscape reconstruction.

This study demonstrates the effectiveness of combining semi-automatic landform classification with erosion and deposition modeling to create a geomorphological map. The advantage of this method is the introduction of a 'digital-first' approach to a region, with only limited fieldwork needed to verify and complement the results. Such an approach allows a geomorphological characterization, including the identification of sediment archives, in regions where fieldwork is challenging for political or other reasons – in our case the Covid-19 pandemic.

Software

The Geomorphons analysis was done using GrassGIS (v.8.3.0). The USPED model was computed in ArcGIS Pro (v.3.1.1). Part of the preparation of the rainfall and soil erodibility factor were done with R. The NDVI was computed with the Google Earth Engine. ArcGIS Pro (v.3.1.1) was used to illustrate the maps and the final map layout was realized in Inkscape (v.1.2.1).

Acknowledgements

We thank our reviewers Walter Chen, Dario Gioia and Luis Tanarro for the constructive comments on the manuscript and map.

This work was written within the project *ISLAMAFR – Conquest, Ecology and Economy in Islamic North Africa: The Example of the Central Medjerda Valley*, a tri-national collaboration between the Institut National du Patrimoine, the Deutsches Archäologisches Institut Berlin, the Freie Universität Berlin and UCL. The project remains indebted to Prof. Faouzi Mahfoudh, Director of the Institut National de Patrimoine for his support.

Disclosure statement

No potential conflict of interest was reported by the author(s).

Funding

The project is funded through a joint grant between the Arts and Humanities Research Council (AHRC) (Project no: AH/T012692/1) and the Deutsche Forschungsgemeinschaft (DFG) (Project no: 429040062).

Data availability

The data that support the findings of this study are available from the corresponding author, J. Pagels, upon reasonable request.

ORCID

Julia Pagels http://orcid.org/0000-0003-1927-5699
Wiebke Bebermeier http://orcid.org/0000-0001-7866-8690

References

Aiello, A., Adamo, M., & Canora, F. (2015). Remote sensing and GIS to assess soil erosion with RUSLE3D and USPED at river basin scale in Southern Italy. *CATENA*, *131*, 174–185. https://doi.org/10.1016/j.catena.2015.04.003

Ardeleanu, S. (2021). Numidia Romana? Die Auswirkungen der römischen Präsenz in Numidien (2. Jh. v. Chr.–1. Jh. n. Chr.) [Dissertation]. Humboldt-Universität, Berlin.

Arnoldus, H. (1977). Methodology used to determine the maximum potential average annual soil loss due to sheet and rill erosion in Morocco (p. 34). FAO Soils Bulletin. https://agris.fao.org/agris-search/search.do?recordid=xf2016048062

Arnoldus, H. (1980). An approximation of the rainfall factor in the universal soil loss equation. In M. de Boodt & D. Gabriels (Eds.), *Assessment of erosion* (pp. 127–132). Wiley.

Arosio, R., Wheeler, A. J., Sacchetti, F., Guinan, J., Benetti, S., O'Keeffe, E., van Landeghem, K. J. J., Conti, L. A., Furey, T., & Lim, A. (2023). The geomorphology of Ireland's continental shelf. *Journal of Maps*, *19*(1), 2283192. https://doi.org/10.1080/17445647.2023.2283192

Arrebei, N., Sabir, M., Naimi, M., Chikhaoui, M., & Raclot, D. (2020). Assessment of soil erosion with RUSLE 3D and USPED in the Nekor Watershed (Northern Morocco). *Open Journal of Soil Science*, *10*(12), 631–642. https://doi.org/10.4236/ojss.2020.1012031

Atkinson, J., de Clercq, W., & Rozanov, A. (2020). Multi-resolution soil-landscape characterisation in KwaZulu Natal: Using Geomorphons to classify local soilscapes for improved digital geomorphological modelling. *Geoderma Regional*, *22*, e00291. https://doi.org/10.1016/j.geodrs.2020.e00291

Ben Ameur, M., Masmoudi, S., & Yaich, C. (2021). Flood and sandstorm events recorded in holocene sebkha deposits in Southeastern Tunisia: Evidence from magnetic and geochemical properties. *Quaternary International*, *571*, 46–57. https://doi.org/10.1016/j.quaint.2020.09.006

Benavidez, R., Jackson, B., Maxwell, D., & Norton, K. (2018). A review of the (Revised) Universal Soil Loss Equation ((R)USLE): With a view to increasing its global applicability and improving soil loss estimates. *Hydrology*

and Earth System Sciences, *22*(11), 6059–6086. https://doi.org/10.5194/hess-22-6059-2018

Beschaouch, A., Hess, U., Khanoussi, M., Kraus, T., Rakob, F., Röder, G., & Röder, J. (1993). *Die Steinbrüche und die antike Stadt* (Vol. 1). von Zabern.

Faust, D., & Wolf, D. (2017). Interpreting drivers of change in fluvial archives of the Western Mediterranean – A critical view. *Earth-Science Reviews*, *174*, 53–83. https://doi.org/10.1016/j.earscirev.2017.09.011

Faust, D., & Zielhofer, C. (2002). Reconstruction of the Holocene water level amplitude of Oued Medjerda as an indicator for changes of the environmental conditions in Northern Tunisia. *Zeitschrift Für Geomorphologie Supplementary Issues*, *128*, 161–175.

Faust, D., Zielhofer, C., Escudero, R. B., & Diaz del Olmo, F. (2004). High-resolution fluvial record of late Holocene geomorphic change in northern Tunisia: Climatic or human impact? *Quaternary Science Reviews*, *23*(16–17), 1757–1775. https://doi.org/10.1016/j.quascirev.2004.02.007

Fenwick, C. (2022). The Arab conquests and the end of ancient Africa? In R. B. Hitchner (Ed.), *A companion to North Africa in antiquity (Blackwell companions to the ancient world)* (pp. 424–438). John Wiley & Sons Inc.

Fenwick, C., Dufton, A., Ardeleanu, S., Chaouali, M., Möller, H., Pagels, J., & von Rummel, P. (2022). Urban transformation in the Central Medjerda Valley (northwest Tunisia) in late antiquity and the middle ages: A regional approach. *Libyan Studies*, *53*, 142–160. https://doi.org/10.1017/lis.2022.17

Ferro, V., Porto, P., & Yu, B. (1999). A comparative study of rainfall erosivity estimation for southern Italy and southeastern Australia. *Hydrological Sciences Journal*, *44*(*1*), 3–24. https://doi.org/10.1080/02626669909492199

Frankl, A., Lenaerts, T., Radusinović, S., Spalevic, V., & Nyssen, J. (2016). The regional geomorphology of Montenegro mapped using land surface parameters. *Zeitschrift Für Geomorphologie*, *60*(1), 21–34. https://doi.org/10.1127/zfg/2016/0221

Gaussen, H., & Vernet, A. (1958). *Carte Internationale du Tapis Végétal. Tunis-Sfax*. Institut Géographique National. Gouvernement Tunisien.

Gießner, K. (1984). Naturraum und landschaftsökologische Probleme: Die Bedeutung des Naturraumes als Entwicklungspotential. In K. Schliephake (Ed.), *Ländermonographien: Vol. 14. Tunesien: Geographie, Geschichte, Kultur, Religion, Staat, Gesellschaft, Bildungswesen, Politik, Wirtschaft* (1st ed., pp. 23–74). Thienemann.

Gioia, D., Danese, M., Corrado, G., Di Leo, P., Minervino Amodio, A., & Schiattarella, M. (2021). Assessing the prediction accuracy of Geomorphon-based automated landform classification: an example from the Ionian coastal belt of Southern Italy. *ISPRS International Journal of Geo-Information*, *10*(11), 725. https://doi.org/10.3390/ijgi10110725

Hengl, T., Mendes de Jesus, J., Heuvelink, G. B. M., Ruiperez Gonzalez, M., Kilibarda, M., Blagotić, A., Shangguan, W., Wright, M. N., Geng, X., Bauer-Marschallinger, B., Guevara, M. A., Vargas, R., MacMillan, R. A., Batjes, N. H., Leenaars, J. G. B., Ribeiro, E., Wheeler, I., Mantel, S., & Kempen, B. (2017). Soilgrids250m: Global gridded soil information based on machine learning. *PLoS One*, *12*(2), e0169748. https://doi.org/10.1371/journal.pone.0169748

Hess, U., Müller, K., & Khanoussi, M. (2017). *Die Brücke über die Majrada in Chimtou* (Vol. 5). Reichert Verlag.

Institut National de la Météorologie. (2018). Les normales climatiques en Tunisie entre 1981–2010. http://data.transport.tn/dataset/normales-climatiques-en-tunisie-1981-2010/resource/acf0d32e-92b3-4247-9281-1b3a1587d23f

Jasiewicz, J., & Stepinski, T. F. (2013). Geomorphons — A pattern recognition approach to classification and mapping of landforms. *Geomorphology*, *182*, 147–156. https://doi.org/10.1016/j.geomorph.2012.11.005

Jebari, S., Berndtsson, R., Bahri, A., & Boufaroua, M. (2010). Spatial soil loss risk and reservoir siltation in semi-arid Tunisia. *Hydrological Sciences Journal*, *55*(1), 121–137. https://doi.org/10.1080/02626660903529049

Jebari, S., Berndtsson, R., Lebdi, F., & Bahri, A. (2012). Historical aspects of soil erosion in the Mejerda catchment, Tunisia. *Hydrological Sciences Journal*, *57*(5), 901–912. https://doi.org/10.1080/02626667.2012.685741

Jemai, S., Kallel, A., Agoubi, B., & Abida, H. (2021). Soil erosion estimation in arid area by USLE model applying GIS and RS: Case of Oued El Hamma catchment, South-Eastern Tunisia. *Journal of the Indian Society of Remote Sensing*, *49*(6), 1293–1305. https://doi.org/10.1007/s12524-021-01320-x

Kefi, M., Yoshino, K., & Setiawan, Y. (2012). Assessment and mapping of soil erosion risk by water in Tunisia using time series MODIS data. *Paddy and Water Environment*, *10*(1), 59–73. https://doi.org/10.1007/s10333-011-0265-3

Khanoussi, M., Kraus, T., Rakob, F., & Vegas, M. (1994). *Der Tempelberg und das römische Lager* (Vol. 2). von Zabern.

Khelil, M., Khomsi, S., Roure, F., Vergés, J., & Zargouni, F. (2021). Structural styles of the Tellian fold-and-thrust belt of Tunisia based on structural transects: Insights on the subsurface oil and gas pre-salt plays. *Arabian Journal of Geosciences*, *14*(19), 1–22. https://doi.org/10.1007/s12517-021-08308-4

Khelil, M., Souloumiac, P., Maillot, B., Khomsi, S., & de Lamotte, D. F. (2019). How to build an extensional basin in a contractional setting? Numerical and physical modelling applied to the Mejerda Basin at the front of the eastern Tell of Tunisia. *Journal of Structural Geology*, *129*, 103887. https://doi.org/10.1016/j.jsg.2019.103887

Kramm, T., Hoffmeister, D., Curdt, C., Maleki, S., Khormali, F., & Kehl, M. (2017). Accuracy assessment of landform classification approaches on different spatial scales for the Iranian Loess Plateau. *ISPRS International Journal of Geo-Information*, *6*(11), 366. https://doi.org/10.3390/ijgi6110366

Lazzari, M., Gioia, D., Piccarreta, M., Danese, M., & Lanorte, A. (2015). Sediment yield and erosion rate estimation in the mountain catchments of the Camastra artificial reservoir (Southern Italy): A comparison between different empirical methods. *CATENA*, *127*, 323–339. https://doi.org/10.1016/j.catena.2014.11.021

Libohova, Z., Winzeler, H. E., Lee, B., Schoeneberger, P. J., Datta, J., & Owens, P. R. (2016). Geomorphons: Landform and property predictions in a glacial moraine in Indiana landscapes. *CATENA*, *142*, 66–76. https://doi.org/10.1016/j.catena.2016.01.002

Mackensen, M., & Baldus, H. R. (2005). *Militärlager oder Marmorwerkstätten: Neue Untersuchungen im Ostbereich des Arbeits- und Steinbruchlagers von Simitthus/Chemtou* (Vol. 3). von Zabern.

Majhi, A., Shaw, R., Mallick, K., & Patel, P. P. (2021). Towards improved USLE-based soil erosion modelling in India: A review of prevalent pitfalls and

implementation of exemplar methods. *Earth-Science Reviews*, *221*, 103786. https://doi.org/10.1016/j.earscirev.2021.103786

Mathieu, M., Nicolas, H., & Castany, G. (1952). *Carte géologique de la Tunisie: Ghardimaou. Feuille No. 31*. Service Géologique de la Direction des Travaux Publics de Tunisie.

Menasria, A., Meddi, M., & Habaieb, H. (2022). Diachronic study of land cover of the Medjerda Watershed and estimation of RUSLE-C factor using NDVI-based equation, remote sensing, and GIS. *Journal of the Indian Society of Remote Sensing*, *50*(3), 451–468. https://doi.org/10.1007/s12524-021-01472-w

Mitasova, H., Barton, M., Ullah, I., Hofierka, J., & Harmon, R. S. (2013). 3.9 GIS-based soil erosion modeling. In J. F. Shroder (Ed.), *Treatise on geomorphology* (pp. 228–258). Academic Press.

Mitasova, H., Brown, W. M., Johnston, L., & Mitas, L. (1996a). GIS tools for erosion/deposition modelling and multidimensional visualization. In *Part II: Unit stream power-based erosion/deposition modelling, and enhanced dynamic visualization* (pp. 4–14). Report for USA CERL, University of Illinois. http://fatra.cnr.ncsu.edu/~hmitaso/gmslab/reports/rep2.ps

Mitasova, H., Hofierka, J., Zlocha, M., & Iverson, L. R. (1996b). Modelling topographic potential for erosion and deposition using GIS. *International Journal of Geographical Information Systems*, *10*(5), 629–641. https://doi.org/10.1080/02693799608902101

Mitasova, H., & Mitas, L. (2001). Multiscale soil erosion simulations for land use management. In R. S. Harmon & W. W. Doe (Eds.), *Landscape erosion and evolution modeling* (pp. 321–347). Springer US.

Mitasova, H., Mitas, L., Brown, W. M., & Johnston, D. M. (1999). Terrain modeling and soil erosion simulations for Fort Hood and Fort Polk test areas. Report for USA CERL, University of Illinois. http://fatra.cnr.ncsu.edu/~hmitaso/gmslab/reports/cerl99/rep99.html

Mitasova, H., Petrasova, A., Petras, V., Warren, S., Hohmann, M., Svendsen, N. G., & Ruzycki, T. (2014). Soil erosion and deposition modeling: GIS-based tutorial. https://ncsu-geoforall-lab.github.io/erosion-modeling-tutorial/index.html

Mosbahi, M., & Benabdallah, S. (2020). Assessment of land management practices on soil erosion using SWAT model in a Tunisian semi-arid catchment. *Journal of Soils and Sediments*, *20*(2), 1129–1139. https://doi.org/10.1007/s11368-019-02443-y

Philip, G. M., & Watson, D. F. (1985). Some limitations in the geostatistical evaluation of ore deposits. *International Journal of Mining Engineering*, *3*(2), 155–159. https://doi.org/10.1007/BF00881627

Rodier, J. A., Colombani, J., Claude, J., & Kallell, R. (1981). Le bassin de la Mejerdah. Monographies Hydrologiques ORSTOM: N°6.

Sandström, S., Markensten, H., Futter, M. N., Kyllmar, K., O'Connell, D. W., Bishop, K., & Djodjic, F. (2023). Distributed dynamic modelling of suspended sediment mobilization and transport from small agricultural catchments. *Frontiers in Environmental Science*, *11*, 1196048. https://doi.org/10.3389/fenvs.2023.1196048

Sharpley, A. N., & Williams, J. R. (1990). EPIC-erosion/productivity impact calculator: 1. Model documentation. Technical Bulletin: No. 1768. US Department of Agriculture.

The EOC Geoservice Team. (n.d.). The TanDEM-X 90 m digital elevation model. https://geoservice.dlr.de/web/dataguide/tdm90/

van der Knijff, J. M., Jones, R., & Montanarella, L. (2000). Soil erosion risk: Assessment in Europe. EUR 19044 EN. European Soil Bureau. https://esdac.jrc.ec.europa.eu/content/soil-erosion-risk-assessment-europe

von Rummel, P., Ardeleanu, S., Beck, D. M., Chaouali, M., & Möller, H. (2019). Simitthus/Chimtou, Tunesien: Die Arbeiten der Jahre 2016 bis 2018. In *E-Forschungsberichte* (pp. 197–205). https://doi.org/10.34780/w4x8-px18

von Rummel, P., Wulf-Rheidt, U., Ardeleanu, S., Beck, D. M., Chaouali, M., Goischke, J., Möller, H., & Scheding, P. (2016). Chimtou, Tunesien: Die Arbeiten der Jahre 2014 und 2015. In *E-Forschungsberichte* (pp. 99–109).

Warren, S. D., & Ruzycki, T. S. (2022). Validation of the USPED erosion and deposition model at Schofield Barracks, O'ahu, Hawai'i. *Pacific Science*, *76*(1), 43–51. https://doi.org/10.2984/76.1.4

Wessel, B. (2018). TanDEM-X ground segment: DEM products specification document. Public Document TD-GS-PS-0021. EOC. https://tandemx-science.dlr.de/

Yang, X., Becker, F., Knitter, D., & Schütt, B. (2021). An overview of the geomorphological characteristics of the Pergamon micro-region (Bakırçay and Madra River Catchments, Aegean Region, West Turkey). *Land*, *10*(7), 667. https://doi.org/10.3390/land10070667

Zielhofer, C., & Faust, D. (2003). Palaeoenvironment and morphodynamics in the mid-Medjerda floodplain (northern Tunisia) between 12 000 and 2000 BP: Geoarchaeological and geomorphological findings. In M. Macklin, D. Passmore, & A. Howard (Eds.), *Alluvial Archaeology in Europe: Proceedings of an International Conference*, Leeds, 18–19 December 2000 (pp. 203–216). AA Balkema.